Assessment of Two Fast Aerodynamic Codes for Guided Projectiles

Ameer G. Mikhail*
U.S. Army Ballistic Research Laboratory, Aberdeen Proving Ground, Maryland

Two fast missile aerodynamic prediction codes, the NSWCAP and Missile DATCOM, have been applied to the geometry of the guided, gun-launched Copperhead projectile. The two codes are evaluated in comparison with wind-tunnel and free-flight range test data. Two configurations are considered for computation: A launch configuration (body-tail) in the Mach range 0.5–1.8 and a maneuvering configuration (body-wing-tail) in the Mach range 0.3–0.95. Results show reasonable agreement for the drag coefficient C_D and very large disagreements for both C_{N_α} and C_{M_α}. Failure to consider both body-slot and fin-gap effects seems to have contributed largely to these differences. The dynamic derivatives C_{ℓ_p} and $(C_{M_q} + C_{M_{\dot\alpha}})$ are not adequately estimated by the NSWCAP Code and are not calculated in the DATCOM Code. For the coefficients actually computed, the DATCOM Code results were slightly more accurate than those of the NSWCAP Code. For both codes, determination of the explicit effects of control surface deflection angles on the aerodynamic coefficients is lacking, a determination that must be made if these codes are to be used as effective prediction tools for guided projectiles. In both codes, several areas of improvement are identified.

Nomenclature

C_D = total drag coefficient, drag force/$0.5\rho_\infty U_\infty^2 S_{\text{ref}}$
C_ℓ = roll moment coefficient, rolling moment/$q_\infty S_{\text{ref}} L_{\text{ref}}$, positive if clockwise (viewed from rear looking forward)
C_{ℓ_p} = $\partial C_\ell / \partial p$
C_M = pitching moment coefficient, pitching moment/$q_\infty S_{\text{ref}} L_{\text{ref}}$ (positive nose up)
C_{M_α} = $\partial C_M / \partial \alpha$, 1/rad
C_n = yawing moment coefficient, yawing moment/$q_\infty S_{\text{ref}} L_{\text{ref}}$ (positive when nose to right)
C_N = normal force coefficient, normal force/$q_\infty S_{\text{ref}}$
C_{N_α} = $\partial C_N / \partial \alpha$, 1/rad
C_Y = side force coefficient
D = body diameter
D_{ref} = body reference diameter
L = body length
L_{ref} = reference length, usually the body diameter
M_∞ = freestream Mach number
P = spin (roll) rate, rad/s
q = pitching motion rate, rad/s
q_∞ = freestream dynamic pressure, $0.5\rho_\infty U_\infty^2$
S_{ref} = reference area, $\pi D^2_{\text{ref}}/4$
t = time
X_{CP} = location of center of pressure, measured from the c.g. toward the base of the projectile
α = angle of attack, positive when producing a positive normal force, deg
α_T = total angle of attack, including sideslip angle, deg
$\dot\alpha$ = $\partial\alpha/\partial t$
δ = fin deflection angle: for fins 1–4, positive when producing a negative (counterclockwise) rolling moment (DATCOM notation); for fins 2 and 4, positive when trailing edge is down (NSWCAP notation)
ϕ = roll orientation angle of the body cross section
ϕ_F = fin orientation angle, measured clockwise from the vertical line of the α_T plane

Presented as Paper 85-4085 at the AIAA 3rd Applied Aerodynamics Conference, Colorado Springs, CO, Oct. 14-16, 1985; received Oct. 28, 1985; revision received July 22, 1986.

*Aerospace Engineer, Launch and Flight Division. Member AIAA.

I. Introduction

SEVERAL fast aerodynamic prediction codes for missiles were written in the last decade. These codes were intended to help missile designers to obtain quick engineering estimates for aerodynamic coefficients and the dynamic stability of their particular configurations.

These fast codes are based on 1) basic and simplified theorems, 2) experimental data that are algebraically or numerically fitted, and/or 3) empirical formulas based on observations and personal experience. The methodology of these codes is based on missile component buildup, with adjustments for component interference (interaction) effects. These codes were required to be fast, usually using less than 60 CPU/s on a typical minicomputer (such as a VAX-11/780) for each flight condition. They were originally meant to give estimates for the basic aerodynamic coefficients, in particular C_D, C_N, C_M, C_{M_α}, C_{N_α}, over a range of Mach numbers and angles of attack.

Now these codes are required to yield more accurate predictions, provide all the aerodynamic coefficients, and cover a larger variety of missile configurations. Application of such missile codes to gun-launched projectiles, both for spin- and fin-stabilized configurations, must also be examined. For such applications, the L/D ratio is usually smaller than that of missiles.

Such codes can be developed to provide more accurate predictions for the increasingly complex projectile and missile configurations. These complex applications require that the following accuracy guidelines be targeted for the basic coefficients:

$$C_D \text{ within} \pm 5\%, \qquad C_{N_\alpha} \text{ and } C_{M_\alpha} \text{ within} \pm 15\%;$$

$$C_{\ell_p} \text{ and } (C_{M_q} + C_{M_{\dot\alpha}}) \text{ within} \pm 25\%$$

These demands for accuracy are more relaxed than the accuracy actually achieved in real tests in the firing ranges, as provided by Rogers.[1] This relaxation is intentional because codes cover a wide variety of body configurations and dif-

ferent speed regimes, where different methods may be used and extrapolation of experimental data may be allowed. Rogers[1] estimates the accuracy of the free-flight measurements as follows:

$$C_D \text{ within} \pm 1\%; \qquad C_{N_\alpha} \text{ within} \pm 5\%$$

$$C_{M_\alpha} \text{ within} \pm 2\%; \qquad (C_{m_q} + C_{m_{\dot\alpha}}) \text{ within} \pm 15\%$$

This accuracy requirement has not been achieved for the present application, as will be discussed in Sec. IV. However, for more traditional configurations in the low supersonic speed regime (Mach number 1.5-2.5), the results are usually more accurate and can fall within the targeted accuracy guidelines.

It is the purpose of this paper to gage the results of the two fast codes based on the results obtained through an application to the hybrid missile-projectile configuration of the Copperhead. The Copperhead projectile is a laser-guided, gun-launched projectile with two sets of spring-out fins. The geometry will be discussed in detail in Sec. II.

The two codes examined are the Naval Surface Weapons Center Aerodynamic Prediction (NSWCAP) Code[2] and the Air Force Missile DATCOM Code.[3] The former code was developed during the 1970s and provided a good tool for design configuration studies. The latter is a more recent code, which makes use of all the methodologies of the former code, with modifications and improvements. The latter code reflects updated theories, includes more recent and accurate experimental data, adds more options for practical missile applications (such as nonaxisymmetric bodies and effects of inlets and rocket motor thrust), and is structured into a more modular form.

Several studies were made by different researchers with regard to the capabilities of several existing fast prediction codes. Some of these codes have narrow capabilities in terms of applicable configurations, flight speed, estimating specific coefficients only, among other restrictions. Reference 4 compares the capabilities and results obtained using MISSILE-2 and DEMON-Series codes. Reference 5 lists and compares some of the methods in ten different codes; among them are the NSWCAP and Missile DATCOM codes. Reference 6 evaluates the NSWCAP and MISSILE-2 codes and refers to several other codes. Reference 7 evaluates methods used for component buildup, which were later used in the Missile DATCOM Code. Reference 8 is a description of the NSWCAP Code, its capabilities, and its analytical techniques as viewed by its authors. Reference 9 is a description of the Missile DATCOM Code with regard to its different methods, as viewed by its principal authors.

It is not the purpose of this paper to survey or compare such a variety of codes but rather to apply two particular codes, which are of a more general nature and which are of interest to the U.S. Army, to a particular hybrid projectile-missile configuration. The objective is to assess the accuracy of these two codes as applied to this particular configuration.

II. Geometry of the Copperhead Projectile

The Copperhead projectile, Fig. 1, has a total length of 54 in. (1371.6 mm) and a diameter of 6.09 in. (155 mm). It has a spherical nose cap and a conical section of semivertex angle of 12.5 deg connecting the nose and the body sections. There is an obturator ring at the end of the body. The base of the projectile is solid, with no holes in it.

The projectile is laser-guided with two sets of spring-out fins. The rear fins (tail) spring out shortly after the projectile leaves the gun tube. The projectile travels in this configuration, usually called the launch configuration, unguided and with a speed decreasing from Mach 1.8 to about 0.95.

The front set of fins (wings) springs out in the subsonic Mach range between 0.95 and 0.80, and the rear control fins

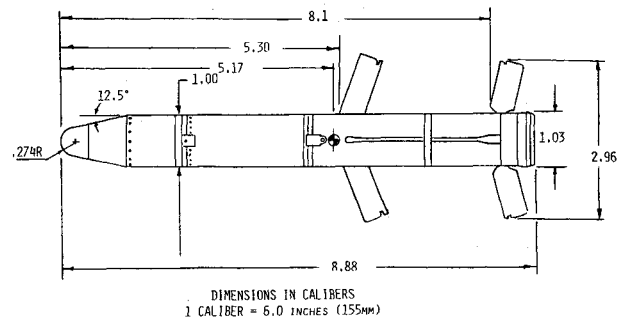

Fig. 1 Configuration of the XM712 Copperhead projectile.

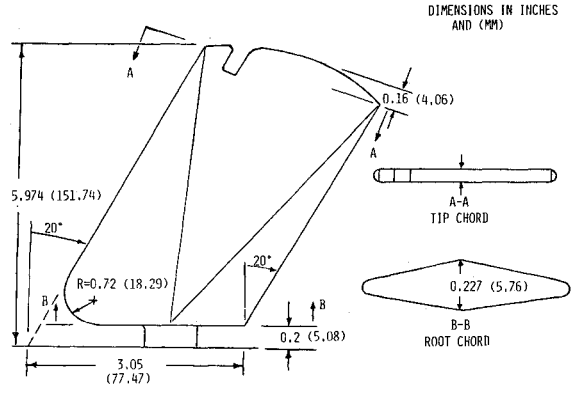

Fig. 2 Copperhead tail fin configuration.

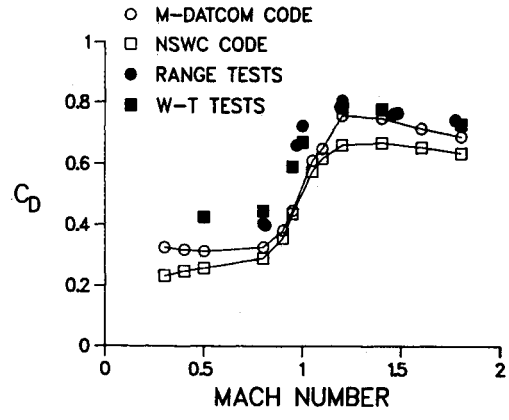

Fig. 3 Total drag coefficient comparison for the launch configuration.

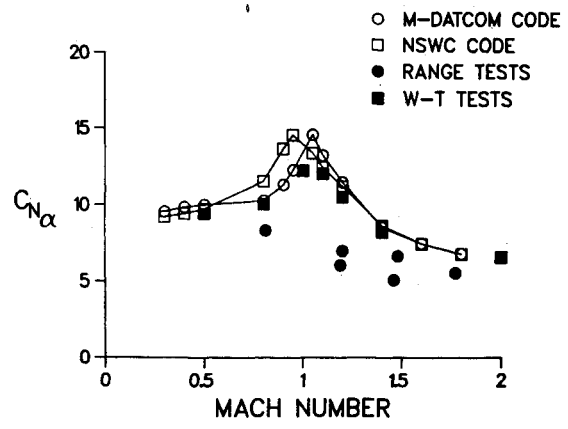

Fig. 4 Normal force slope comparison for the launch configuration.

(tail) are then activated to guide the projectile to its target. The projectile is said to be in its maneuvering configuration at this Mach range, with both wing and tail fin sets deployed.

The rear fin geometry is shown in Fig. 2. The fin is swept back 20 deg and is tapered in thickness from the root to the tip sections. The cross section near the root is diamond-shaped with leading- and trailing-edge rounding. The fins are controlled through stems, with 0.2-in. (5.08-mm) clearance between the body and the fin root.

The front fins (wings) are similar to the tail fins with two exceptions. First, the semispan length is 7.149 in. (181.6 mm) compared to 5.974 in. (147.2 mm) for the tail fins. Second, there is no gap between the fin root section and the projectile body surface.

Both sets of fins have slightly different shapes of slots in the projectile body, where they are housed before deployment. Both sets of fins have tip notches for the releasing mechanisms to hold the fins before they are sprung out from their housing locations.

III. Application of the Codes

Both codes were applied for sea-level conditions with a Reynolds number of 6.18×10^6/Mach number/ft.

Both codes were applied for both launch and maneuvering configurations in the range of Mach number $0.3 \leq M \leq 1.8$. Some modifications in the fin geometry had to be made to suit the input capability of each code. For example, the fin-swept tip chord had to be made horizontal and the semispan was adjusted to account for that. Also, the tail-fin body gaps were not considered, and the tail fins were assumed to extend continuously to the root section. Moreover, the details of the obturator were ignored, and the obturator was modeled as if it were a small "bump" on the body, with a certain height as is usually the case for simulating a "rotating band." The zero-lift case was always computed, in addition to the small angle-of-attack case ($\alpha = 2$ deg).

IV. Results and Comparisons

Free-flight data are available in Ref. 10, while wind-tunnel results were obtained from Ref. 11.

Launch Configuration

First, four flight conditions were chosen from Ref. 10, and both codes were run at Mach numbers and angles of attack of 1.77, 2.9 deg; 1.47, 1.8 deg; 1.20, 1.1 deg; and 0.81, 0.9 deg. The results for C_D, C_{M_α}, C_{N_α}, and X_{CP} are considered reasonable. The results of $(C_{M_q} + C_{M_{\dot\alpha}})$ as obtained by NSWCAP is largely inaccurate, especially for $M = 0.8$. For subsonic speeds, the NSWCAP Code does not compute $C_{M_{\dot\alpha}}$; therefore, the value of $(C_{M_q} + C_{M_{\dot\alpha}})$ is not properly calculated in that speed regime. In fact, for the case of $M = 0.81$, $\alpha = 0.9$ deg, the range result showed an unstable

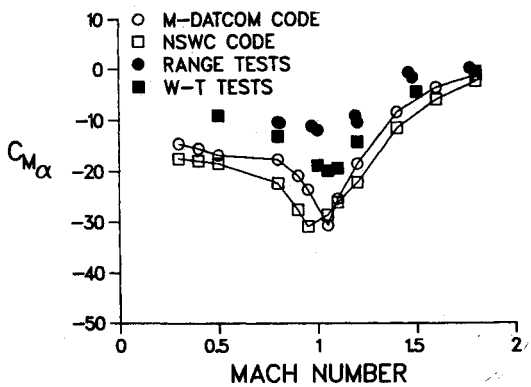

Fig. 5 Pitching moment slope comparison for the launch configuration.

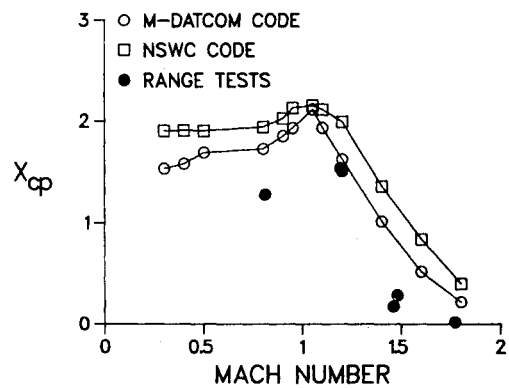

Fig. 6 Location of center of pressure for the launch configuration.

Table 1 Comparison of code results with measured data; launch configuration (B-T)

Mach no.	Angle of attack	Prediction method	C_D	C_{M_α} (c.g.) rad^{-1}	$C_{N_{\alpha_1}}$ rad^{-1}	X_{CP} (cal-base)	$(C_{M_q} + C_{m_{\dot\alpha}})$ s/rad
$M = 1.77$	$\alpha = 2.9$ deg	Range test results[a]	0.740	−0.06	5.51	3.69	−99
		NSWC Code	0.654	−2.930	7.253	3.30	−210.12
		DATCOM Code	0.698	−1.77	6.915	3.454	—[b]
$M = 1.47$	$\alpha = 1.8$ deg	Range test results[a]	0.760	−0.88	5.07	3.53	−200
		NSWC Code	0.671	−9.606	8.445	2.56	−228.9
		DATCOM Code	0.733	−6.648	8.073	2.89	—[b]
$M = 1.20$	$\alpha = 1.1$ deg	Range test results[a]	0.803	−10.52	6.96	2.24	−132
		NSWC Code	0.663	−22.14	11.33	1.74	−248.6
		DATCOM Code	0.746	−18.53	11.35	2.08	—[b]
$M = 0.81$	$\alpha = 0.9$ deg	Range test results[a]	0.398	−10.56	8.31	2.43	15
		NSWC Code	0.296	−22.78	11.88	1.78	−252.8
		DATCOM Code	0.320	−18.14	10.33	1.95	—[b]

[a]From Ref. 10. [b]DATCOM code does not compute this coefficient.

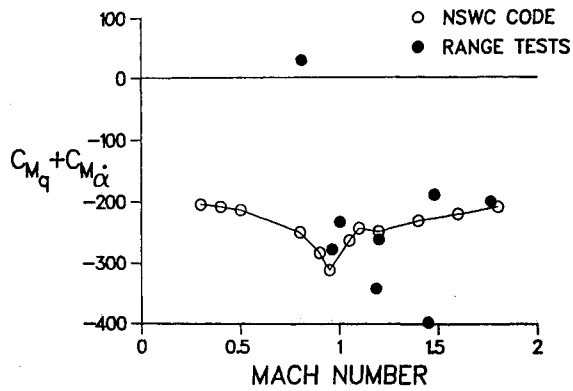

Fig. 7 Pitch damping coefficient comparison for the launch configuration.

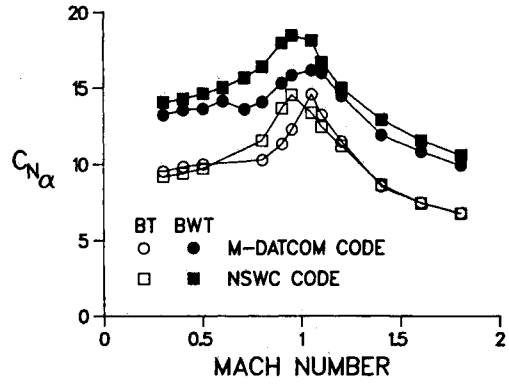

Fig. 9a Normal force slope coefficient for both launch and maneuver configurations.

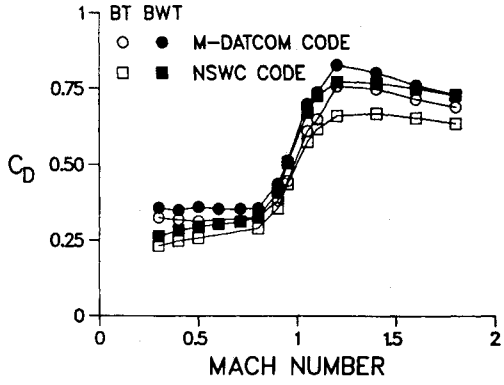

Fig. 8 Total drag coefficient for both launch and maneuver configurations.

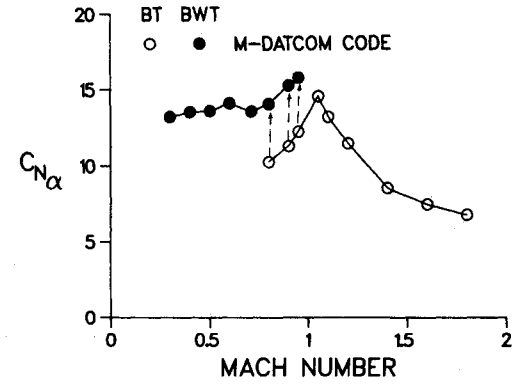

Fig. 9b Change in normal force slope coefficient from launch to maneuver configuration.

flight condition based on pitch damping, although the code predicted a stable condition. Range data are compared to the computed results in Table 1.

Second, the two codes were applied in the Mach range 0.3–1.8 at zero angle of attack. The results for C_D are shown in Fig. 3. Both codes underpredict the wind-tunnel and range data. This may be expected because of failure to consider the effects of the fin slots of the projectile body in both codes. Also body-fin clearance (gap) effects, which should be applied to the tail fins, are not considered in either code. In addition, the DATCOM Code does not include the obturator effect, which is usually modeled as a rotating band. The computed results of both codes agree better with the experimental data in the supersonic regime ($M>1.2$), worsen in the transonic regime ($M=0.8$–1.2), and deteriorate further at subsonic speeds ($M<0.8$).

Reference 12 reported the effects of fin slots on the normal and axial forces of the Copperhead. Wind-tunnel tests were made on a full-scale projectile at both subsonic ($M=0.5$) and supersonic ($M=1.5$) speeds.

References 13–16 also reported the effects of body slots. Such information should be used for future modeling in both codes. Also, Ref. 15 suggests a modification to account for the fin-body gap (clearance) effects.

Figure 4 shows the slope of the normal force C_{N_α} as it varies with the Mach number. The two codes gave close values to each other, but they both overpredicted considerably the range results in the transonic regime between Mach numbers 0.8 and 1.2. It is surprising that the wind-tunnel results are also significantly higher than those of the free-flight range tests. The normal force predictions of the codes can be improved if both fin-gap and body-slot effects are accounted for and when an average roll orientation angle is considered.

Figure 5 shows the slope of the pitching moment about the c.g. Consistent with the overprediction of C_{N_α}, both codes overpredict the pitching moment slope. The predictions are three times larger than free-flight data. The DATCOM Code is closer to the experimental data than the NSWCAP, due to better prediction of the location of the center of pressure. The observation made earlier, that the wind-tunnel data was considerably higher than the range data, is also evident here.

Figure 6 shows the DATCOM results for the X_{CP} location to be more accurate than those of NSWCAP. Compared to free-flight data of Ref. 10, the DATCOM results are more accurate but still overpredict X_{C_P}, by about 0.4 caliber.

Figure 7 shows the NSWCAP predictions for the pitch damping coefficient. The DATCOM Code, on the other hand, does not compute this derivative. The trend shown agrees with the range results only in the supersonic Mach range down to $M\simeq 1.2$. It is suggested that the unsteady pitch damping coefficient $C_{M_{\dot{\alpha}}}$ is largely in error, possibly due to fin flutter or to unsteady flow effects in and out of the body slots and around fin-body gaps, which are not considered in the code. However, for transonic and subsonic speeds, the code fails to predict the trend as well as the magnitude. Omission of $C_{M_{\dot{\alpha}}}$ for those speed regimes is a possible reason for such failure.

Maneuvering Configuration

With the wing fins deployed, the projectile decelerates from Mach 0.95 to 0.3. Computations were made, however, for this B-W-T configuration for the Mach range 1.8–0.3.

Figure 8 shows the total drag coefficient for this configuration in comparison to the launch configuration (B-T). The increase in drag is due to wing fin drag less the reduction in drag due to the interference of the wing fins on the tail fins. The DATCOM Code shows a smaller increase than

Table 2 NSWCAP Code results for roll damping coefficient, C_{ℓ_p} 3(Rad/s)$^{-1}$

Launch configuration (B-T), $\delta = 0$ deg, $\alpha = 0$ deg							
Mach no.	0.5	0.8	0.9	0.95	1.2	1.5	1.8
NSWCAP Code	−14.07	−15.84	−19.06	−20.16	−20.65	−14.6	−11.32
Wind tunnel	−10.50	−11	−11.4	−12	−16	−11.1	−9.8
Maneuvering configuration (B-W-T), $\delta = 0$ deg, $\alpha = 0$ deg							
Mach no.	0.5	0.8	0.9	0.95	1.2	1.5	1.8
NSWCAP Code	−34.97	−38.74	−45.0	−47.0	−50.92	−38.5	−30.49
Wind tunnel	−20	−22	−23.5	−24.2	−28	−25.2	−23

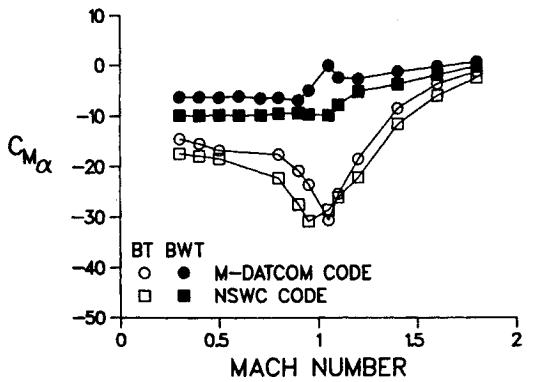

Fig. 10a Pitching moment slope for both launch and maneuver configurations.

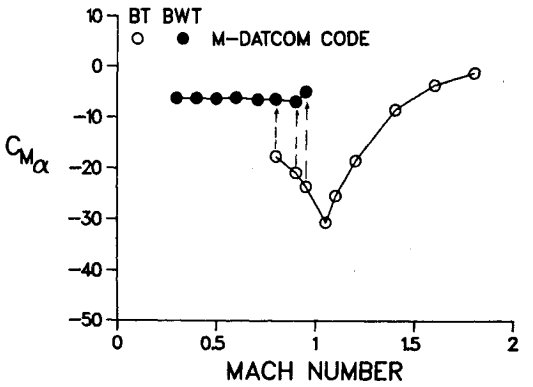

Fig. 10b Change in pitching moment slope from launch to maneuver configuration.

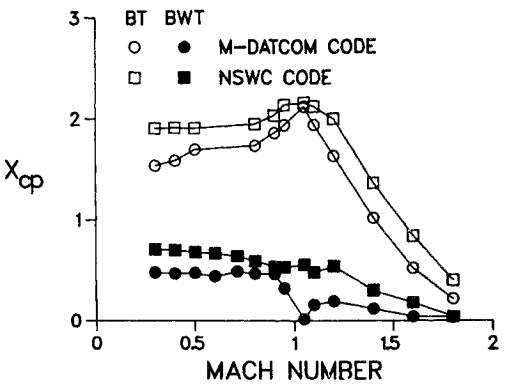

Fig. 11a Location of center of pressure for both launch and maneuver configurations.

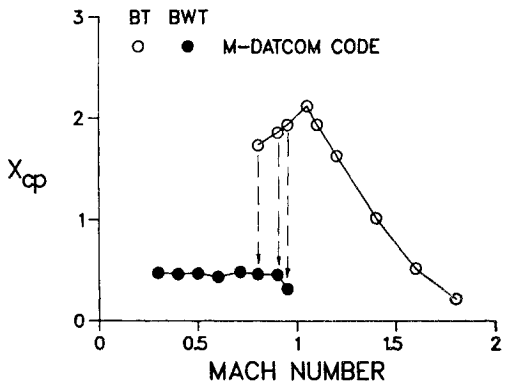

Fig. 11b Change in location of center of pressure from launch to maneuver configuration.

that of the NSWCAP Code, due to vortex tracking corrections included in DATCOM, while the larger effect, as computed by the NSWCAP, is due to lack of consideration of wing-tail interference effects. It should be pointed out that a recent nonlinear vortex-tracking procedure has been developed[17] and has demonstrated more accurate predictions.

Figure 9a shows the normal force slope, where the increase caused by the wing fin lift is smaller for the DATCOM Code than the increase predicted by the NSWCAP Code. The cause for this is the reduction in lift of the tail fin due to the trailing vortex of the wing, as accounted for in the DATCOM Code. Figure 9b shows the change in normal force slope as predicted by the DATCOM Code, due to the deployment of the wing fins. Three Mach numbers (0.95, 0.9, and 0.8) were chosen for the projectile speed at the time of deployment of the wing fins.

Figure 10a shows the pitching moment slope for a range of Mach numbers. For the B-W-T configuration, the wing normal force pushes the center of pressure forward toward the nose, causing the pitching moment about the c.g. to be smaller. Thus, the projectile is less stable. Figure 10b displays a decrease in the static stability of the projectile due to the reduction in pitching moment slope from −25. to −5. The location of the center of pressure X_{CP} is shown in Fig. 11a to shift toward the c.g. and away from the projectile base. Figure 11b shows the sudden shift in the location of the X_{CP} due to wing deployment.

The dynamic stability for pitch disturbance remains almost unchanged for the B-W-T configuration (compared to the B-T) in the supersonic regime as predicted by the NSWCAP Code and shown in Fig. 12. The DATCOM Code, on the other hand, does not compute this derivative. The trend shown agrees with the range results only in the supersonic Mach range down to $M \simeq 1.2$. It is proposed that the unsteady pitch damping coefficient $C_{M_{\dot{\alpha}}}$ is largely in error, possibly as a result of fin flutter or of unsteady flow effects in and out of the body slots and around fin-body gaps, which are not considered in the code. However, for transonic

Table 3 Capability comparison and areas of needed development

	NSWCAP Code	Missile DATCOM Code
	I. Fins	
1a	Only 2 or 4 fin panels in cruciform "plus" position only	Only 2 or 4 fin panels[a], arbitrary roll angle
1b	No roll angle aerodynamics	Arbitrary roll orientation
2	Limited to two sets of fins	Limited to two sets of fins[b]
3	No body fin-slot effects	No body fin-slot effects
4	No fin-body gap effects	No fin-body gap effects
5	No fin side-sweep angle effects	No fin side-sweep angle effect
6	No interdigitated wing and tail fins	Interdigitated wing and tail fins
7	Some aft-body fins corrections	No aft-body fins
8	Linear wing-tail interference	Includes improved vortex correction for downwash effects
9	No wraparound fins	No wraparound fins
10	Limited fin cross-section geometry options	Limited fin cross-section geometry options
11	Gives erroneous results for perfect delta fin (or close to perfect delta planform)	Gives much worse results for perfect delta fin (or close-to-perfect delta planform)
12	Only tip and root fin cross sections specified	Multifin cross-section geometries can be specified (max of 10)
13	Assumes parallel line of sources for fin geometry	Does not assume parallel line of sources for fin geometry
14	Does not include lifting surface nonlinearity at high angle of attack	Includes the equivalent angle of attack for nonlinearity at high α
	II. Body Aerodynamics	
1a	Computes base pressure drag	Computes base pressure drag but does not add it to axial or drag forces
1b	Base pressure drag deteriorates at large α (>10 deg) (overpredicted)	Base pressure drag is not function of α
2	No surface roughness or grooving effects	Includes surface roughness, but no grooving effects
3	Includes rotating band contribution to C_D	Does not include rotating band effect on C_D
4	Calculates high Mach number cases for blunt nose	Does not accept any nose bluntness at high supersonic speeds ($M=4$–5)
5	Yields fair blunt-nose hypersonic aerodynamics ($M>3$)	Yields very poor blunt-nose hypersonic aerodynamics ($M>3$)
6	Yields poor subsonic and transonic blunt-nose aerodynamics ($M<1.2$)	Yields fair subsonic and transonic blunt-nose aerodynamics
7	No forebody vortex shedding effects	No forebody vortex shedding effects
8	No intermediate body vortex shedding effects	No intermediate body vortex shedding effects

	NSWCAP Code	Missile DATCOM Code
	III. Vehicle (Body and Fins) Dynamics	
1	Computes roll damping C_{ℓ_p} and pitch damping $(C_{M_q}+C_{M_{\dot\alpha}})$ coefficients	Does not compute any dynamic derivatives[c]
2	$C_{M_{\dot\alpha}}$ is not computed for subsonic or transonic speeds ($M\leq 1.2$) (set to zero)	
3	$(C_{M_q}+C_{M_{\dot\alpha}})$ is not adjusted to include effects of deflection angle of fins (i.e., it remains constant with δ)	
4	C_{ℓ_p} is fairly computed for one set of fins only; however, it is largely in error for wing-tail combination (no wing-tail interference effects)	
	IV. Fin Control	
1	Only two fins allowed pure pitching; no simultaneous yawing or combined yawing/pitching	Independent four-fin deflection angles
2	No expressions or derivatives for control surface effectiveness; (C_{N_δ}, C_{M_δ})	No expressions or derivatives for control surface effectiveness (C_{N_δ}, C_{M_δ})
3	$(C_{M_q}+C_{M_{\dot\alpha}})$ is not corrected for δ (remains constant with variations in δ)	$(C_{M_q}+C_{M_{\dot\alpha}})$ is not calculated
4	C_{N_α} (and C_{M_α}) for any case with fin deflection is calculated as $C_N/\Delta\alpha$, and is void when $\alpha=0.0$	No difficulty in computing C_{N_α} and C_{M_α} for configurations with control surface deflection
	V. General Features	
1	Takes about 40 CPU/s for a single Mach number and angle of attack (on a VAX-11/780)	Faster by a factor of 1.5 (approximately)
2	Accepts a single angle of attack, and performs a loop for up to 20 Mach numbers	Accepts several Mach numbers and performs a loop for angles of attack (minimum of two) for each Mach number
3	Has no difficulty with redundant input data	Gives erroneous results if redundant (but consistent) input data is given
4	Uses input in ft only (combined with some input in calibers)	Can use in., ft, cm, or m

[a] Arbitrary number of fins capability is now being added to the newer version of the code. [b] A third set of fins is being added in the newer version of the code. [c] Presently being added in the newer version of the code.

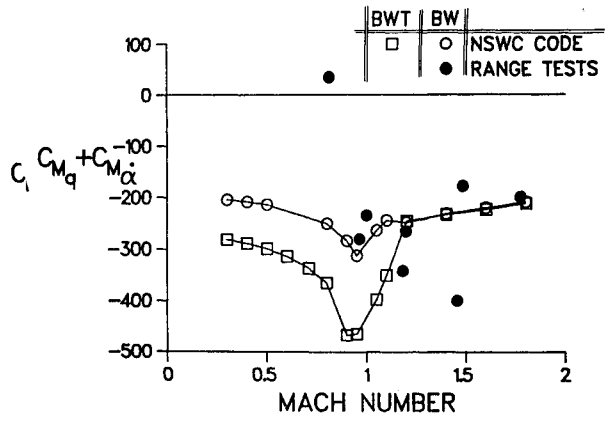

Fig. 12 Pitch damping coefficient for both launch and maneuver configurations.

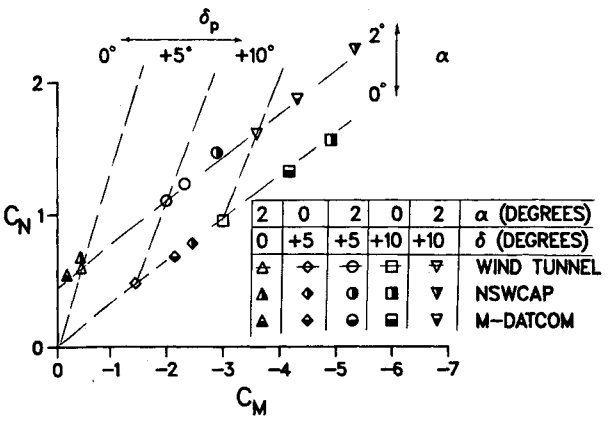

Fig. 14 Maneuver configuration longitudinal stability at $M=0.95$.

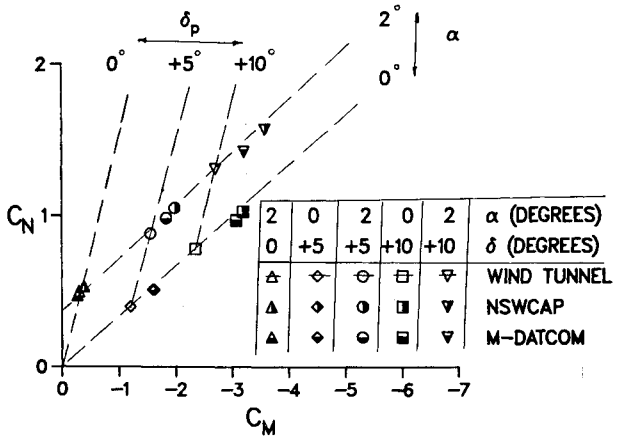

Fig. 13 Maneuver configuration longitudinal stability at $M=0.5$.

and subsonic speeds, the code fails to predict the trend as well as the magnitudes. Omission of $C_{M_{\dot\alpha}}$ for those speed regimes seems to be a possible reason for such failure.

Figure 13 shows the longitudinal stability chart for small α and moderate tail deflection angles δ at Mach number 0.5. It is shown that the NSWCAP Code overpredicts both C_M and C_N for all cases more than the DATCOM Code does. For the same α, the discrepancy increases with the increase in δ. Similar results are also shown in Fig. 14 for Mach number 0.95. It is noticed that the discrepancy increased for this transonic speed, as shown earlier in Figs. 4 and 5 for C_{N_α} and C_{M_α}. The DATCOM Code predicts better results than the NSWCAP, especially for large δ, due to the inclusion of the equivalent angle of attack approach of Ref. 17.

The roll damping coefficient was computed for both configurations only by the NSWCAP Code since the DATCOM Code does not presently have this capability. The results for B-T configuration are shown in Table 2, where reasonable agreement with the wind-tunnel results can be observed, especially when the transonic speed range is excluded. However, the predictions become extremely large for the B-W-T configuration, and this is attributed to lack of consideration of wing-tail interference effects C_{ℓ_p} in that code.

V. Areas of Needed Development

Table 3 lists areas of needed development in both codes. This list was compiled through the application to the Copperhead projectile case and other cases. The order in which areas are listed does not reflect their order of importance, which varies according to the needs and objectives of each user.

VI. Conclusions

Through the application of the two codes—NSWCAP and Missile DATCOM—to the Copperhead projectile geometry, the following conclusions have been drawn:

1) The DATCOM Code generally gave slightly better results, compared with experiment, than those of the NSWCAP.

2) Both codes badly estimated the slopes of the normal force and pitching moment coefficients from failure to include fin-slot and fin-gap effects in either code.

3) The effects of the deflection angles of the control surfaces are not explicitly computed in either code. Both codes failed to provide this information, which is essential to guided-projectile configurations.

4) The dynamic derivatives of the NSWCAP Code are not accurate for this configuration in the transonic and subsonic regimes. Furthermore, they are not calculated in the present version of the DATCOM Code.

5) Both codes gave poor estimates for all aerodynamic coefficients in both the subsonic ($M<0.8$) and transonic ($0.8<M<1.2$) speed regimes.

6) The DATCOM Code, developed more recently, is written in a modular form, allowing ease of modification and checking. The NSWCAP, as a pioneer code, lacks this feature.

7) Areas of needed development in both codes were identified and noted herein for future development.

Finally, these codes serve an important function and should be further developed to meet users' needs.

References

[1]Rogers, W. K., "The Transonic Free Flight Range," U.S. Army Ballistic Research Laboratory, Aberdeen Proving Ground, Maryland, BRL Rept. 1044, June 1958. (AD 200177)

[2]Devan, L. and Mason, L. A., "Aerodynamics of Tactical Weapons to Mach Number 8 and Angle of Attack 180°: Part II—Computer Program and User's Guide," NSWC TR 81-358, Sept. 1981.

[3]Vukelich, S. R., "Automated Missile DATCOM: Vol. 1—Program User's Guide," McDonnell-Douglas Corp. Report, St. Louis, MO, Aug. 1984.

[4]Dillenius, M. F. et al., "Comprehensive Missile Aerodynamics Programs for Preliminary Design," AIAA Paper 82-0375, Jan. 1982.

[5]Williams, J. E. Jr., "Evaluation of Supersonic Missile Aerodynamic Prediction Techniques," AIAA Paper 82-0390, Jan. 1982.

[6]Sun, J. and Cummings, R. M., "Evaluation of Missile Aerodynamic Characteristics Using Rapid Prediction Techniques," *Journal of Spacecraft and Rockets,* Vol. 21, Nov.-Dec. 1984, pp. 513-520.

[7]Vukelick, S. R. and Jenkins, J. E., "Evaluation of Component Build Up Methods for Missile Aerodynamic Predictions, *Journal of Spacecraft and Rockets,* Vol. 18, Nov.-Dec. 1982, pp. 481-488.

[8]Devan, L., Sun, J., and Moore, F. G., "Aerodynamic Prediction for Tactical Weapons," AIAA Paper 79-0361, Jan. 1979.

[9]Vukelich, S. R. and Jenkins, J. E., "Missile DATCOM: Aerodynamic Prediction of Conventional Missile Using Component Build-Up Techniques," AIAA Paper 84-0388, Jan. 1984.

[10]McCoy, R. L., "Free Flight Range Tests of the Copperhead Projectile," U.S. Army Ballistic Research Laboratory, Aberdeen Proving Ground, Maryland, ARBRL-MR-03090, March 1981. (AD A100274)

[11]Appich, W. H. and Wittmeyer, R. E., "Summer 1978 —Aerodynamic Simulation Model Update: Full Scale Model Data (XM-939)," Martin-Marietta Corp., Rept. No. ANA 960000-010, Sept. 1978.

[12]Appich, W. H. Jr. and Wittmeyer, R. E., "Aerodynamic Effects of Body Slots on a Guided Projectile with Cruciform Surfaces," *Journal of Spacecraft and Rockets,* Vol. 17, Nov.-Dec. 1980, pp. 522-528.

[13]Washington, W. D., Wittmeyer, R. E., and Appich, W. H. Jr., "Design Approach for Estimating Body Slots Effects on Wing-Body-Tail Lift," *Journal of Spacecraft and Rockets,* Vol. 18, Nov.-Dec. 1981, pp. 481-482.

[14]Washington, W. D., Wittmeyer, R. E., and Appich, W. H. Jr., "Body Slots Effects on Wing-Body and Wing-Tail Interference of Typical Cannon Launched Guided Projectile," AIAA Paper 80-0260, Jan. 1980.

[15]Sun, J., Hanson, S. G., Cummings, R. M., and August, H., "Missile Aerodynamics Prediction (MAP) Code," *Journal of Spacecraft and Rockets,* Vol. 22, Nov.-Dec. 1985, pp. 605-613.

[16]Appich, W. H. Jr., McCoy, R. L., and Washington, W. D., "Wind Tunnel and Flight Test Comparisons for a Guided Projectile with Cruciform Tails," AIAA Paper 80-0426, Jan. 1980.

[17]Hemsch, M. J. and Nielsen, J. N., "The Equivalent Angle of Attack Method for Estimating the Non-Linear Aerodynamic Characteristics of Missile Wing and Control Surfaces," *Journal of Spacecraft and Rockets,* Vol. 20, July-Aug. 1983, pp. 356-362.